Available online at www.sciencedirect.com

ScienceDirect

Procedia CIRP 46 (2016) 307 – 310

www.elsevier.com/locate/procedia

7th HPC 2016 – CIRP Conference on High Performance Cutting

A Bi-Criterion Flexible Registration Method for Fixtureless Inspection of Compliant Parts

Kaveh Babanezhad[a,*], Gilles Foucault[a], Antoine Tahan[b], Jean Bigeon[a]

[a]*Univ. Grenoble Alpes, Lab. G-SCOP UMR5272, F-38000 Grenoble, France*
[b]*Ecole de Technologie Superieure, 1100 Notre-Dame West, Montreal H3C 1K3, Canada*

* Corresponding author. Tel.: +33-4-76574840. *E-mail address:* kaveh.babanezhad@g-scop.grenoble-inp.fr

Abstract

Manufactured mechanical parts such as sheet metal and thin-wall featured parts, often have significant geometrical differences compared to their nominal CAD models as they have a considerably different shape in a free state condition due to gravity and/or residual stress. Thus, expensive conformation fixtures are traditionally used during inspection operations. Naming such parts flexible (non-rigid or compliant), in this paper, a new method for avoiding fixtures is introduced. Validation was conducted on a virtual industrial case study typically produced with waterjet cutting. Obtained satisfactory results reflect the effectiveness and utility of this approach in precision detection of manufacturing defects.

Peer-review under responsibility of the International Scientific Committee of 7th HPC 2016 in the person of the Conference Chair Prof. Matthias Putz

Keywords: Metrology; Surface analysis; Alignment; Optimization

1. Introduction

Manufactured mechanical parts often have geometrical differences compared to their nominal CAD models and are often inspected for these differences during quality control. This inspection is typically performed in two steps: First, preliminary geometric data of the part in its state-of-use position (usually in the form of scanned point clouds or stereolithography (STL) files) are gathered. Next, the gathered data are processed using computer-aided inspection tools (CAI) designed to identify location and magnitude of a number of manufacturing defects (profile tolerance). Though this twofold inspection routine has gained considerable popularity, it is currently limited to parts that are reasonably rigid. Some parts such as skins, parts with thin walls, which are referred to as flexible (or nonrigid or compliant), have a considerably different shape in a free state compared to their nominal CAD models due to the effect of gravity and/or residual stress. In fact, the geometric deviation of flexible parts is mostly due to such elastic deformations rather than manufacturing defects. As a result, to correctly identify all or the majority of defects, traditionally, one is required to first set up standard or specialized conformation fixtures that would hold the part in the position defined in its nominal CAD model. It is only then that it becomes possible to gather the preliminary geometric data of the part for subsequent analysis in CAI software. A number of downsides exists in using fixtures such as: their time consuming set-up process, considerable acquisition and operation expenses, limitations of standard fixtures in some scenarios, etc. Disadvantages of this sort have led researchers to try to circumvent use of fixtures by digitally deforming (or better called *registering*) the gathered point cloud data of a flexible part in Euclidean space until it matches the part's corresponding nominal CAD model, thereby elastically deforming the data to reach an optimal assembly shape whilst avoiding neutralization of any existing manufacturing defect. In this paper the same goal is pursued as a hypothesis to investigate whether a *flexible* registration method for nonrigid transformation of preliminary point cloud data onto nominal shapes can be introduced or not.

A summary of the recent advancements and research trends in the field (automated inspection of freeform surfaces) are well presented in details in [1], accompanied with specific definitions, notions, and challenges of dealing with flexible

Peer-review under responsibility of the International Scientific Committee of 7th HPC 2016 in the person of the Conference Chair Prof. Matthias Putz
doi:10.1016/j.procir.2016.04.023

parts. The literature that is directly related to the focus of this paper however, three dimensional point cloud registration methods, can be divided into two main categories: methods of rigid registration, and methods of nonrigid registration. Rigid registration approaches can only perform linear translations and rotations in the Euclidian space and as a result are not usable in the problematic of this study as the deviated shape of a flexible part's point cloud will not change (deform) under these linear operations. The second category, nonrigid registration approaches, is divided into quite a number of sub-categories ranging from semi-nonrigid methods restricted to affine transformations (shear, scale, etc.), to fully nonrigid (in a sense free-form deformation) methods capable of registering point clouds to almost any shapes given the right inputs were to be provided. Although introduction of all these sub-categories far exceeds the limits of this publication, a recent concise survey reviewing them is available in [2]. As for the purposes of this paper, the preference has been the Coherent Point Drift algorithm (CPD) [3] which is of state of the art status already adopted by many, and can register point clouds to almost any shapes. Despite the fact that nonrigid registration methods such as CPD can succeed where rigid registration methods fail (deforming point clouds), they are initially designed for applications such as registering medical images and have no regard for preserving the intrinsic material properties of the scanned part during the registration process (properties such as curvilinear distances, mesh size parameters, geodesic distance between nodes, etc.) and thus create unrealistic results which are not reliable for defect identification purposes (since such registrations in real life would in fact either add additional stress to the part or in some cases tear the material apart). To solve this issue, a new branch of nonrigid registration methods needs to be developed that would respect such intrinsic material properties during registration. We refer to these type of methods as *flexible* registration methods. It is also noteworthy to mention other types of deficiencies that most nonrigid registration methods often have: a lack of entirely automatic behavior (end-user is required to set key tuning parameters), a lack of automatic approximation of the noise/outliers level (even if the algorithm possesses dedicated tuning parameters to neutralize them), a costly runtime when registering large point clouds, etc. The only standalone flexible pointwise registration algorithm that has been introduced so far, to the knowledge of the authors, is that of Aidibe et al. [4] named Adapted CPD algorithm (ACPD). Whilst using the CPD algorithm at its core, the ACPD algorithm introduced a singular cost function composed of weighted sum of two elements to be minimized: First being a scalar distance criterion representing the average pointwise Euclidean distances between the source (scan data) and target (nominal CAD) point clouds. And second, an isometry conservation criterion representing the change in the average geodesic distance between each vertex to its neighbors on the point cloud after registration (similar to a criterion first described in [5]). By minimizing this cost function, ACPD algorithm attempts to conduct an optimal flexible registration that would respect the material properties of the source point cloud. This algorithm however, has some limitations such as: reliance on the end-user to provide the weights inside the cost function, not guaranteed to find the global optima, and not being accurate within its distance calculation in cases where the target point cloud data is incomplete. In this paper, a more generalized flexible registration method (and an algorithm based on it) is introduced that by design not only covers the limitations of ACPD, but also will introduce new capabilities. Resulting contributions include: a generalized wrapper based on the methodology that could be expanded to include future nonrigid registration algorithms and not remain limited to CPD, automatic selection of the tuning parameters of the nonrigid registration algorithm, implicit noise handling, a better route to optimality via using a bi-objective formulation as opposed to a singular formulation, and improving the distance calculation between the source and target point clouds. The algorithm developed based upon the proposed method has been named *BOFR1* where the acronym stands for the **1**st version of a **B**i-**O**bjective **F**lexible **R**egistration algorithm.

2. Methodology

As mentioned in section 1, the aim of this work is to develop a flexible registration method for compliant parts and an algorithm based upon it. The concept behind this method is *bi-objectively optimizing two key criteria that are the output of a black-box containing a nonrigid registration algorithm inside*. Main steps of the developed method (very similar to the code structure of BOFR1 algorithm) are presented in Fig. 1.

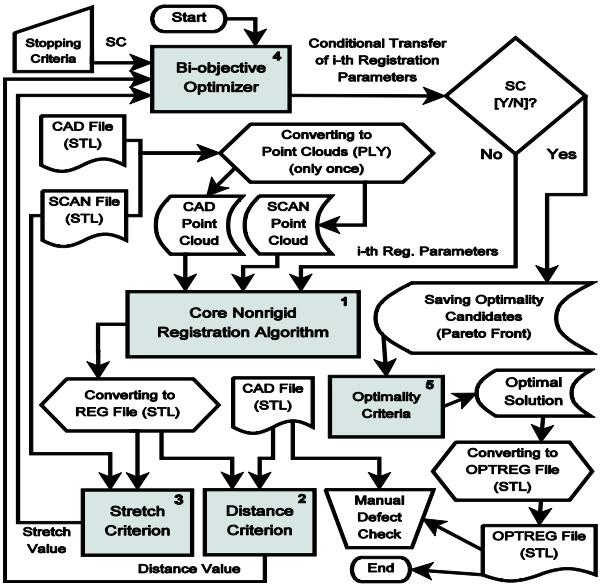

Fig. 1. Main steps of the proposed method

Theoretically, any branch of nonrigid registration algorithms capable of performing a free-form alike deformation can be used within the aforementioned black-box (block 1 in Fig. 1). In BOFR1, the latest version (v2.0) of the original CPD algorithm [3] was chosen. Motivations for this decision are the state of the art status of the CPD algorithm, its relatively good efficiency in registering large point clouds compared to other options, and an internal noise-canceling ability should the end-user manages to tune it properly. The inputs of the black-box (containing CPD) which are optimized include registration parameters λ and β, and noise handling parameter ω (enabling implicit noise handling in BOFR1). As for the optimization solver (block 4), BiMADS algorithm [6] was picked due its general superiority to a weighted single-objective scheme, its

deterministic behavior (as opposed to a stochastic search), its efficiency in bi-objectivity handling and approximation of 2D Pareto fronts whilst satisfying some necessary optimality conditions (and as a result insuring with a predefined level of confidence the finding of a global optima), and its ability to work with black-boxes. The first of the two outputs of the black-box to be minimized (block 2), referred to as the distance criterion, calculates the Hausdorff distance between the source and the target triangular meshes (named REG and CAD respectively in Fig. 1), after each registration process in the optimization loop. Let $RV = \{v_{r1}, v_{r2}, \dots, v_{rn} | v_{ri} \in \mathbb{R}^3\}$ be the set of n vertices extracted from the source mesh file (REG), $CV = \{v_{c1}, v_{c2}, \dots, v_{cn'} | v_{ci} \in \mathbb{R}^3\}$ be the set of n' vertices extracted from the target mesh file (CAD), $RT = \{t_{r1}, t_{r2}, \dots, t_{rm} | t_{rj} \in \mathbb{R}^{3x3}\}$ be the set of m triangles belonging to the source mesh file (REG) where each t_{ri} contains vertices' coordinates of the *i-th* triangle, and similarly $CT = \{t_{c1}, t_{c2}, \dots, t_{cm'} | t_{cj} \in \mathbb{R}^{3x3}\}$ be the set of m' triangles belonging to the target mesh file (CAD). A *directed* source-to-target mesh Hausdorff distance ($h(RV, CT)$) could then be described as the *« maximum vertex-to-triangle distance of the set RV to the nearest triangle in the set CT »*. In mathematical form it can be written as:

$$h(RV, CT) = \max_{v_{ri} \in RV} \{ \min_{t_{cj} \in CT} dist(v_{ri}, t_{cj}) \} \quad (1)$$

where $dist$ is a function programed to calculate the distance between a vertex and a triangle. Similarly, a directed target-to-source Hausdorff distance can be calculated and denoted by $h(CV, RT)$. The *two-way* or *cumulative* Hausdorff distance (referred to in this paper only as the Hausdorff distance) would be defined as:

$$H_d(RV, CT) = \max \{ h(RV, CT), h(CV, RT) \} \quad (2)$$

H_d is the distance criterion used as one of the cost functions in the optimization loop. A small value for the distance criterion is an indicator of a satisfactory superimposition of the source mesh onto the target mesh. For an absolutely perfect superimposition, this value would be equal to zero. The second of the two outputs of the black-box to be minimized (block 3), referred to as the stretch criterion, is the same as what was proposed in [4] and provides a cumulative measure of the change in the average of geodesic distances (equal to mesh sizes) between each vertex to its neighbors on the same mesh (SCAN in Fig. 1) after the mesh has been registered to a new shape (REG in Fig. 1) during the optimization process. Let RV and RT be the same sets defined in the description of the distance criterion. The stretch differences δ_S and stretch criterion Δ_S are then respectively presented as:

$$\delta_S = N^{-1} \left| \sum_{i=1}^{N} D_{R,i} - \sum_{i=1}^{N} D_{S,i} \right| \quad (3)$$

$$\Delta_S = \sqrt{\frac{\sum \|\delta_S\|^2}{n-1}} \quad (4)$$

where N is the number of neighbors around vertex v_{ri}, $D_{R,i}$ is the average distance between v_{ri} and its neighbors, and Δ_S is the Euclidean norm of differences in δ_S between the initial (SCAN) and the registered (REG) mesh. A small value for the stretch criterion indicates that the trialed registration step has not significantly changed the average of distances between mesh vertices to their neighbors. A stretch criterion equal to zero indicates a perfect conservation of such distances. Amongst other remaining steps, the role of the optimality criterion (block 5), once the bi-objective optimization solver has converged, is to determine which member of the resulting two dimensional Pareto frontier is the best pick. Given that the two elements of the bi-objective cost function were the scalar distance and stretch values, each member of this two dimensional plot has coordinates composed of distance and stretch criteria. In BOFR1, the Pareto member with the smallest stretch assigned to it will be picked. However, in cases where the difference between the minimum and maximum of stretch values are insignificant (e.g. if the less than 1×10^{-3} mm), the Pareto member with the smallest City Block distance (Manhattan distance) from the origin [0,0] will be picked.

3. Results

In order to validate the claims of the proposed methodology and demonstrate achieved improvements over previous methods, BOFR1 and ACPD have been tested against a virtually created case study from the aerospace industry. To clarify, a virtual case study is comprised of a CAD model of an industrial part (volumetric/solid geometry) that is then modified to contain a number of defects. This modified version of the CAD model is then deformed using a finite element software package (where the part is mounted from one side and deviates due to simulated gravity) and subsequently saved as a deformed solid body, acting as a virtual scan of the part in its free state condition. This is followed by extracting one of the key surfaces of both the nominal CAD model and the virtual scan (representing the surface that would have been scanned in a real world scenario by a human operator), and exporting them in STL format after a meshing operation (surface meshing). Finally, a simulated measurement noise in Gaussian form is added to the STL mesh of the virtual scan (in per-vertex average normal directions). Concerning this study, SolidWorks was used to modify the nominal CAD shape of the case study part (i.e. for adding defects and simulating gravity), and Mefisto-Mesher (via FreeCAD) was used to create the aforementioned surface meshes. Testing against a virtual case study as a validation approach makes it possible to numerically assess the developed algorithm's effectiveness and utility. In this context, BOFR1 and ACPD are both applied to the case study, and the registered meshes they result in (OPTREG, see Fig. 1) are saved in STL format. For a global performance comparison of BOFR1 and ACPD, studying the distance criterion value (eq. 2) associated with the two algorithms' OPTREG output mesh reveals which one has achieved a better superimposition between source and target meshes of the case study. Similarly, comparing the corresponding stretch differences matrices (eq. 3) shows which algorithm has better respected the intrinsic material properties of the part during registration. Furthermore, though the main focus of this paper is on flexible registration rather than identification of manufacturing defects in scanned parts, nine instances of potential contour (profile 2D) defects were added to the virtual case study and their magnitudes were later *manually* measured by comparing the aforementioned OPTREG output meshes and the nominal CAD mesh of the case study in PolyWorks CAI software. An illustration of these defects which can be categorized under two types (holes' center

offset, and internal cut-outs' offset) are depicted in Fig. 2-a. Naturally, a negligible difference between the measured defect value and the known actual value of that artificial defect in the virtual case study means a satisfactory estimation of the defect magnitude has been achieved. Thus, by association, the effectiveness of BOFR1 and ACPD in estimating defect magnitudes can be quantified and compared. In order for either the global performance comparison or defect magnitude estimation capability to be properly utilized as a sensible comparison metric, a set of *validation assumptions* and *conditions* were anticipated and followed during the creation of the virtual case study. The validation assumptions are: *measurement noise amplitude is smaller than of the added defects*, and *areas affected by defects do not cover the majority of the parts surface area*. The sole validation condition to be respected is: *during the process of creating a solid body from the deformed finite element mesh, errors induced in curvilinear dimensions must be smaller than the maximum production tolerances of the part in reality*. The mechanical part of the chosen virtual case study comes from the aerospace industry, where waterjet cutting is often used in production and profile tolerance ranges are between 0.8 to 1.2 millimeters. The profile tolerance range in our case was picked to be 1 millimeter and the previously mentioned error in the curvilinear dimensions in the created virtual scan remained well below this tolerance range and therefore it has not affected the results significantly. Also, it is noteworthy to mention that the profile tolerances of the case study part are without any constraints (6 degrees of freedom) and are analyzed in accordance with ISO-1101 2012 standards (equivalent to ASME-Y14.5 2009) as all-over specifications without any datum referencing. The measurement noise added to the virtual scan of the case study was equal to 25 microns, accounting for a laser scanner that would have been used in reality to capture the scanned point cloud. Laser scanners in the aerospace industry are often mounted on a robot manipulator or a coordinate measurement machine (as opposed to being held by hand) which in turn results in an equipment accuracy of approximately 10 to 20 microns. Thus, for the numerical assessment of algorithm performances and reporting results, the appearance resolution was chosen to be 10 times smaller than the aforementioned equipment accuracy, which equals to 1 micron. A top view of the virtual case study is depicted in Fig. 2-b. The part was divided into three zones with three potential defect instances in each. Defects in zone B have a magnitude of zero microns and were defined as such in the virtual scan to quantify possible over-estimations of defect magnitudes.

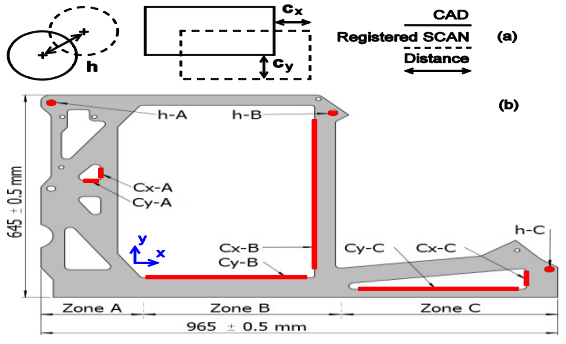

Fig. 2. (a) Defects and analyzed dimensions, (b) Top-view of the case study

Regarding the case study's data size, the source point cloud (SCAN.ply, see Fig. 1) contained 18348 points whilst the target (CAD.ply) contained 18327. Results of the numerical assessment of BOFR1 are presented in Table 1 and Table 2.

Table 1. Global performance comparison of BOFR1 & ACPD

Global Comparison Metric (**in micrometers**)	Value	
	ACPD	BOFR1
Max. of the absolute stretch differences δ_S	**44**	**1**
Average of the absolute stretch differences δ_S	**6**	**0**
Hausdorff distance between OPTREG and CAD (see Fig. 1), calculated similarly via H_d (see eq. 2)	**3333**	**1133**

Table 2. Defect magnitude estimations (see Fig. 2 for description of defects)

Defects (**in micrometer**)		Zone A	Zone B	Zone C
Hole (**h**)	actual magnitude	**300**	**0**	**800**
	ACPD estimation	**431**	**263**	**2548**
	BOFR1 estimation	**309**	**77**	**803**
Cut-out	actual magnitude	**300 / 300**	**0 / 0**	**800 / 800**
(**c_x / c_y**)	ACPD estimation	**313 / 302**	**1437 / 19**	**2568 / 797**
	BOFR1 estimation	**307 / 310**	**31 / 9**	**814 / 812**

4. Conclusion

In this paper, a new methodology was proposed to deal with the problematic of fixtureless inspection of flexible parts, which is a real concern in the industry due to the costs it imposes. An algorithm (BOFR1) was developed and tested on a virtual industrial case study. Satisfactory results reflected on the algorithm's capability and precision. Adequate estimation of defect magnitudes demonstrated the potential of the approach for quality control purposes, and in turn forecasting the mount-ability of parts in an assembly. Future work to be undertaken include: benchmarking the methodology on more case studies (BOFR1 has only been tested on quasi-planar parts), and development of fully automated defect identification tools to calculate defect magnitudes as opposed to the manual measurements conducted in this study via CAI software.

References

[1] G.N. Abenhaim, A. Desrochers, A. Tahan, Nonrigid parts' specification and inspection methods: Notions, challenges, and recent advancements, Int. J. Adv. Manuf. Technol. 63 (2012) 741–752. doi:10.1007/s00170-012-3929-2.

[2] G.K.L. Tam, Z.-Q. Cheng, Y.-K. Lai, F.C. Langbein, Y. Liu, D. Marshall, et al., Registration of 3D Point Clouds and Meshes: A Survey from Rigid to Nonrigid, IEEE Trans. Vis. Comput. Graph. 19 (2013) 1199–1217. doi:10.1109/TVCG.2012.310.

[3] A. Myronenko, X. Song, Point Set Registration, Coherent Point Drift, IEEE Trans. Pattern Anal. Mach. Intell. 32 (2009) 2262–2275. doi:10.1109/TPAMI.2010.46.

[4] A. Aidibe, A. Tahan, Adapting the coherent point drift algorithm to the fixtureless dimensional inspection of compliant parts, Int. J. Adv. Manuf. Technol. (2015). doi:10.1007/s00170-015-6832-9.

[5] L. Klein, T. Wagner, C. Buchheim, D. Biermann, A procedure for the evaluation and compensation of form errors by means of global isometric registration with subsequent local reoptimization, Prod. Eng. 8 (2014) 81–89. doi:10.1007/s11740-013-0510-2.

[6] C. Audet, G. Savard, W. Zghal, Multiobjective optimization through a series of single-objective formulations, SIAM J. Optim. 19 (2008) 188–210. doi:10.1137/060677513.